International Journal of Cardiology 281 (2019) 150–155

Contents lists available at ScienceDirect

International Journal of Cardiology

journal homepage: www.elsevier.com/locate/ijcard

Quantification of doxorubicin-induced interstitial myocardial fibrosis in a beagle model using equilibrium contrast-enhanced computed tomography: A comparative study with cardiac magnetic resonance T1-mapping

Zhen Zhou [a,1], Lei Xu [a,*,1], Rui Wang [a,1], Akos Varga-Szemes [b,1], James A. Durden [b,1], U. Joseph Schoepf [b,1], Zhonghua Sun [c,1], Zhanming Fan [a,1]

[a] Department of Radiology, Beijing Anzhen Hospital, Capital Medical University, Beijing, China
[b] Division of Cardiovascular Imaging, Department of Radiology and Radiological Science, Medical University or South Carolina, Charleston, SC, USA
[c] Department of Medical Radiation Sciences, Curtin University, Perth, WA 6845, Australia

ARTICLE INFO

Article history:
Received 16 October 2018
Received in revised form 12 December 2018
Accepted 4 January 2019
Available online 15 January 2019

Keywords:
Equilibrium contrast-enhanced computed tomography
Cardiac magnetic resonance imaging
Diffuse interstitial myocardial fibrosis
Extracellular volume fraction
Serum fibrosis index

ABSTRACT

Background: The noninvasive equilibrium contrast-enhanced cardiac computed tomography (CCT) has potential for myocardial tissue characterization. The objective of this study was to test the feasibility of CCT-based extracellular volume (ECV) fraction in beagle models of doxorubicin-induced interstitial myocardial fibrosis, with cardiac magnetic resonance (CMR) as the reference.

Methods: This study was approved by local ethics committee. Thirteen beagles were included with ECV quantified by CCT and CMR at baseline, 16 and 24 weeks after modeling. Spearman correlation analysis was used to determine the association between CT ECV, CMR ECV, collagen volume fraction (CVF), LVEF and serum fibrosis index (Hyaluronic acid [HA], Laminin [LN] and Type-III procollagen [PCIII]).

Results: Median ECV values in CT and CMR at 16 and 24 weeks were significantly higher than those at baseline (CT ECV: 34.4% and 37.7% vs. 25.2%; CMR ECV: 32.2% and 37.4% vs. 22.7%; $P < 0.001$). A strong correlation was found between CCT and CMR for ECV ($r = 0.899$, $P < 0.001$). Both correlated well with CVF ($r = 0.951$ and 0.879 for CT and MR ECV vs. CVF, $P < 0.001$), serum fibrosis index ($r = 0.830$–0.907 for CT and MR ECV vs. HA, LN, PCIII, respectively, $P < 0.05$) and were inversely related to LVEF ($r = -0.846$ and -0.804 for CCT and CMR, $P < 0.001$). Bland-Altman analysis showed a small bias (1.5%), with 95% limits of agreement of −2.7% and 5.6%.

Conclusions: CCT-derived ECV correlates well with CMR, histology and serum fibrosis index, suggesting that CCT is capable of myocardial tissue characterization.

1. Introduction

Diffuse interstitial myocardial fibrosis refers to a variety of quantitative and qualitative changes in the myocardial interstitial collagen network that occur in various cardiomyopathies [1]. Cardiac toxicity is the most serious adverse effect of anthracycline drugs, which can cause interstitial myocardial fibrosis and adverse cardiac events [2]. Since Arheden et al. firstly described the method of determination of extracellular volume (ECV) fraction on CMR, T1-mapping with contrast medium-enhanced cardiac magnetic resonance (CMR) imaging has been increasingly used to assess the diffusely abnormal myocardium [3,4]. Myocardial ECV fraction, derived from CMR T1 measurements represents the equilibrium distribution of gadolinium in the myocardium and blood [4–6]. CMR T1-mapping-based ECV measurement has been validated in a variety of conditions, such as ischemic cardiomyopathies, valvulopathy, myocarditis and non-ischemic cardiomyopathies [7–11]. However, CMR has its own shortcomings such as the long scanning time, the scanner-related costs and certain typical MR-specific contraindications (e.g. metal implants, or claustrophobia, etc.) [12].

Recently, cardiac computed tomography (CCT) has also been used to detect diffuse myocardial fibrosis based on the attenuation difference of the myocardium and blood between pre- and post-contrast CT images. The attenuation change can be used to calculate ECV, which is similar to

Abbreviations: CMR, cardiac magnetic resonance; ECV, extracellular volume fraction; LVEF, left ventricular ejection fraction; Hct, hematocrit; LN, Laminin; CCT, cardiac computed tomography; CVF, collagen volume fraction; LGE, late gadolinium enhancement; HA, Hyaluronic acid; PCIII, Type-III procollagen.

* Corresponding author at: Department of Radiology, Beijing Anzhen Hospital, Capital Medical University, No. 2 Anzhen Rd, Chaoyang District, Beijing 100029, China.
E-mail address: leixu2001@hotmail.com (L. Xu).

[1] This author takes responsibility for all aspects of the reliability and freedom from bias of the data presented and their discussed interpretation.

https://doi.org/10.1016/j.ijcard.2019.01.021
0167-5273/

the effect of gadolinium agents used in CMR [13]. The feasibility of myocardial ECV measurements with CCT has been evaluated in animal models. Jablonowski et al. and Hong et al. showed good performance of CT-derived ECV in detecting diffuse myocardial fibrosis in pig and rabbit models [14,15]. However, Jablonowski et al. evaluated the accuracy of CT-derived ECV only in myocardial ischemia and infarction models. The small heart size and the fast heart rate (HR) or arrhythmia of the rabbits used in Hong et al. by dual-Energy CT might have limited the quantitative assessment of myocardial fibrosis. Further evidence is required to verify the reliability of CT-derived ECV.

The objective of this proof of concept study was to test the feasibility of equilibrium contrast-enhanced cardiac computed tomography (CCT)-based ECV fraction assessment against CMR T1 mapping-based ECV measurements in a beagle model of doxorubicin-induced interstitial myocardial fibrosis.

2. Methods

2.1. Animal model and experimental workflow

This study was approved by the Animal Care and Use Committee at the [***BLINDED***] and followed the ARRIVE guidelines. Fifteen female beagles weighing 8 to 10 kg were included. Three of them were sacrificed for histological evaluation before the doxorubicin administration (Pre-modeling), while the other beagles (n = 12) received 30 mg/m^2 intravenous doxorubicin (Doxorubicin hydrochloride, D8740, Solarbio, Beijing, China) at every 3 weeks, until a cumulative dose of 240 mg/m^2 was reached [16]. Doxorubicin was diluted in 20 ml of 0.9% normal saline and slowly infused intravenously. Two animals in the doxorubicin group died from acute heart failure prior to reaching their target cumulative dose. At 16 weeks after the start of the doxorubicin intervention, the surviving dogs (n = 10) underwent same day CCT and CMR scans. Subsequently, 3 beagles were sacrificed to obtain histological evaluation. The rest of the dogs (n = 7) underwent additional CCT and CMR scans at 24 weeks, and were then sacrificed for histological assessment (Fig. A.1).

2.2. Animal preparation for CCT and CMR

Beagles were examined by CCT and CMR before doxorubicin administration (pre-modeling) and at the end of 16 and 24 weeks after modeling. Anesthesia was induced using an intramuscular injection of a mixture of xylazine hydrochloride (2.0 mg/kg) and ketamine hydrochloride (1.0 mg/kg). Before CCT and CMR, a forelimb vein of each dog was prepared for intravenous contrast agent administration and blood was collected to measure the hematocrit (Hct) value and serum fibrosis index.

2.3. Equilibrium contrast-enhanced CCT protocol

All subjects were examined with a CT system (Somatom Definition Flash, Siemens Healthcare, Forchheim, Germany). The CCT protocol included an initial survey scan, pre-contrast, and post-contrast CT scans after a scan delay of 5 min, 10 min and 15 min. The parameters used for the pre-contrast CT scan were as follows: tube voltage, 100 kV with automatically selected tube current; slice thickness, 0.6 mm; delay 2 s. Iterative reconstruction (SAFIRE, Siemens) was used to improve image quality with a strength of 3 and reconstruction increment of 0.4 mm. The post-contrast CT scan was performed after intravenous infusion of 1.5 ml/kg iodinated contrast (370 mg iodine/ml, Ultravist, Bayer Schering Pharma, Berlin, Germany) and 20 ml normal saline at a rate of 2 ml/s by using the parameters identical to those of the pre-contrast CT scan. The first post-contrast scan started at 5 min, and additional scans were performed at 10 and 15 min after contrast injection, respectively.

2.4. CMR protocol

CMR was performed on the same day of the CCT scan. All beagles were examined using a 3.0 T MR scanner (Magnetom Verio, Siemens Healthcare, Erlangen, Germany) with a 32-channel cardiovascular array coil (Vivo, Orlando, Fla). Cine, pre-contrast and post-contrast T1-mapping images were acquired along with late gadolinium enhancement (LGE) images. In order to analyze cardiac function, cine steady-state free precession (SSFP) sequences were acquired in long-axis 4-chamber and short-axis views to cover the whole left ventricle. Scanning parameters were as follows: TR 45.6 ms, TE 1.66 ms, field of view 219 mm × 260 mm, matrix 256 × 256 pixels, slice thickness 4 mm for long-axis 4-chamber images and 6 mm for short-axis views, spatial resolution 1.0 × 0.9 mm^2, flip angle 50°, and average acquisition time 20 s per slice. T1-mapping acquisition of a long-axis 4-chamber view was performed with a modified Look-Locker inversion recovery sequence (MOLLI, 5(3)3 scheme, SSFP readout) both before and 15 min after gadopentetate dimeglumine (15 ml:7.04 g, Beilu, Beijing, China) was injected at a rate of 2 ml/s followed by a 10 ml saline flush. The following parameters were used: TR 351.2 ms; TE 1.14 ms; field of view 222 mm × 260 mm; slice thickness 4 mm; and matrix 150 × 192 pixels, resulting in a spatial resolution of 1.7 × 1.2 mm^2, flip angle 35°; and average acquisition time 9 s per slice. Eight minutes after the injection of the contrast agent, LGE images were acquired using a magnitude and phase-sensitive inversion recovery-prepared SSFP sequence. The LGE scan parameters were as follows: TR 577 ms, TE 1.67 ms, FOV 211 mm × 260 mm, matrix 156 × 256 pixels, slice thickness 4 mm for long-axis 4-chamber images and 6 mm for short-axis views, spatial resolution 1.6 × 1.0 mm^2, flip angle 20°, and average acquisition time 10 s per slice.

2.5. Image quality evaluation

Based on visual assessment of image artifact and delineation between the left ventricle myocardium and cavity, the image quality of the myocardial CT images and T1-maps were subjectively classified as good (no artifacts, clear demarcation, unstinted evaluation), adequate (minimal or moderate artifacts, slightly influenced evaluation), or poor (severe artifacts that apparently affected diagnostic confidence).

2.6. CCT image analysis

Two observers (R.W. and Z.Z. with 6 and 5 years of experience in cardiac imaging, respectively), blinded to each beagle's findings, repeatedly performed pre-contrast and post-contrast measurements in order to calculate CT-derived ECV on a commercial workstation (Syngo MMWP; Siemens). Regions of interest (ROIs) were manually drawn at the septal and lateral segments of the left ventricle myocardium and inside the left ventricle cavity (avoiding papillary muscles) in order to obtain attenuation values (Fig. 1). CCT-derived ECV was calculated using the following formula:

$$ECV = \left(\frac{\Delta HU_{myo}}{\Delta HU_{blood}}\right) \times (1-Hct)$$

where ΔHU_{myo} and ΔHU_{blood} are the differences between myocardium and blood attenuation (Hounsfield units, HU) values before and after contrast administration [15]. Effective radiation doses of CT scans were calculated by using a conversion factor of 0.014 mSv/mGy·cm [17].

2.7. CMR image analysis

Long-axis 4-chamber view CMR images were chosen to manually draw ROIs in accordance with CCT ROIs on a dedicated workstation (Syngo, Siemens) (Fig. A.2). ROIs were carefully drawn to avoid partial volume averaging along the myocardium/blood interface [12]. The mean T1 value in each ROI was recorded and ECV fraction was calculated according to the following formula [4,8]:

$$ECV = \left(\frac{1}{T1_{post\text{-}myo}} - \frac{1}{T1_{pre\text{-}myo}}\right) \div \left(\frac{1}{T1_{post\text{-}blood}} - \frac{1}{T1_{pre\text{-}blood}}\right) \times (1-Hct)$$

where $T1_{pre\text{-}myo}$ and $T1_{post\text{-}myo}$ are the T1 values of the myocardium before and after the administration of gadolinium-based contrast agent (GBCA), while $T1_{pre\text{-}blood}$ and $T1_{post\text{-}blood}$ are the T1 values of blood before and after contrast. The basic parameters of cardiac function, including end-diastolic volume (EDV), end-systolic volume (ESV), stroke volume (SV), cardiac output (CO), and left ventricular ejection fraction (LVEF), were manually analyzed in short-axis views of LV using the Siemens Syngo Argus commercial software.

2.8. Serum fibrosis index analysis

Venous blood (5 ml) was collected to measure the serum fibrosis index immediately before the CCT and CMR scans. Serum separation was conducted within 24 h and the serum was stored in a refrigerator at −20 °C. Radioimmunoassay (RIA) was used to test the levels of chronic serum fibrotic markers (HA, LN and PCIII).

2.9. Histological analysis

After the CCT and CMR examinations, samples from the LV of each beagle were collected and fixed in 10% formalin for histology. After dehydration and embedding, sectioning was performed at a slice thickness of 5 μm followed by Masson's trichrome staining. A digital histology slide scanner (Pannoramic MIDI, 3D HISTECH, Budapest, Hungary) was used to digitalize specimen slides. Quantitative assessment was conducted using a histology image analysis software (Quant center, 3D HISTECH). To calculate collagen volume fraction (CVF), ROIs were manually drawn on the Masson's trichrome-stained digital histology images in accordance with the CT and MR ROIs, and then the average CVF of the slice was calculated [18]. A pathologist with 10 years of experience was responsible for analyzing the histological data in Kang PuAn Biotechnology Co. Ltd. (Beijing, China).

2.10. Statistical analysis

Data were analyzed using statistical software (SPSS 25.0, Chicago, ILL). Continuous data were presented as mean ± SD, and categorical variables were described as frequencies or percentages. Spearman correlation analysis was used to determine the association among CT-derived ECV, CMR-derived ECV, CVF, pre-T1 values, serum fibrosis index and LVEF. The Bland-Altman plots were used to compare the agreement between CT-derived ECV and CMR-derived ECV. The change in CT-derived ECV, MR-derived ECV, pre-T1 values, serum fibrosis index and CVF were evaluated according to the modeling time (among pre-modeling, 16 weeks and 24 weeks after modeling), while the change in CT-derived ECV

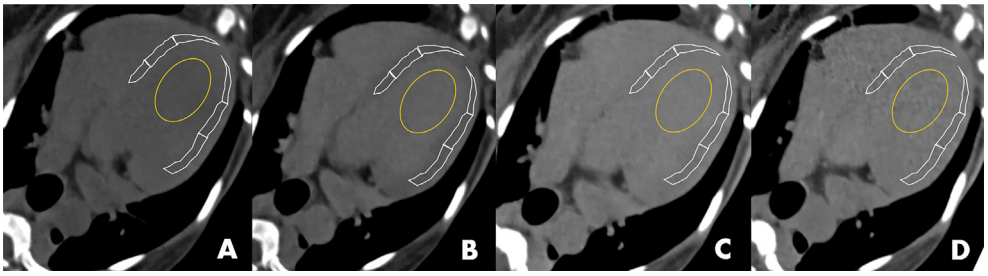

Fig. 1. Examples of myocardial CT images. Regions of interest are drawn in the septal and lateral segments of left ventricle on pre-contrast (A) and post-contrast (B, at 5 min, C, at 10 min and D, at 15 min after contrast administration) CCT images (white: myocardium; orange: blood).

values were evaluated according to the scan time (5 min, 10 min and 15 min after contrast injection) by a linear mixed model. The linear mixed model included fixed effects for time and random effects for each subject. Time was considered as a categorical variable in the model and the covariance was assumed to be equal among all time points. Interobserver agreement was assessed using the intraclass correlation coefficient (ICC). The receiver operating characteristic curve (ROC curve) was reconstructed to compare the CT-derived ECV, MR-derived ECV, serum fibrosis index (HA, LN and PCIII) and EDV with that of LVEF for the diagnosis of post-modeling subjects [19]. $P < 0.05$ is recognized as statistical difference.

3. Results

3.1. Characteristics of beagles

The beagles' characteristics are summarized in Table 1. The mean body weight was 8.4 ± 1.4 kg for the pre-modeling group, 7.1 ± 1.2 kg for the study group of 16 weeks and 8.8 ± 0.8 kg for 24 weeks modeling. The Hct level and LVEF decreased with the elongation of modeling time while the left ventricular volume (LVV) of the beagles increased (16-week group vs. pre-modeling group, $P < 0.05$; 24-week group vs. pre-modeling group, $P < 0.05$). The mean CT radiation dose of each subject was 5.62 ± 1.59 mSv.

3.2. Quality of cardiac CT images and T1 maps

We analyzed a total of 720 LV segments of CCT images. Of these, 648 segments (90.0%) met the diagnostic requirements. Results showed that 488 segments (67.8%) were good (score = 3), 160 segments (22.2%) were adequate (score = 2), and 72 segments (10.0%) were poor (score = 1). And 360 LV segments were analyzed for both pre T1 and post T1 maps images. Of these, 258 segments (71.7%) were good (score = 3), 72 segments (20.0%) were adequate (score = 2), and 30 segments (8.3%) were poor (score = 1). The poor segments were eliminated from the image analysis.

3.3. Comparison of CCT ECV with CMR ECV

Detailed ECV results are provided in Table A.1. ECV increased with the duration of doxorubicin injection (Median (P25, P75) of CT ECV: pre-modeling group, 16-week group and 24-week group were 25.2% (22.7%, 25.6%), 34.4% (33.4%, 35.3%) and 37.7% (36.6%, 37.9%), respectively; corresponding MR ECV values were: 22.7% (21.3%, 23.8%), 32.2% (31.6%, 34.0%) and 37.4% (33.3%, 39.1%), respectively). ECV was statistically different between the groups (all $P < 0.05$). However, CT ECV measurements showed no significant difference among scans performed at 5 to 15 min after contrast administration (Table A.2). A good correlation was found between CT-derived ECV and MR-derived ECV across all subjects ($n = 30$; $r = 0.899$; $P < 0.001$). The Bland-Altman plots showed small bias between CT and MR-derived ECV (1.5%) with 95% limits of agreement from −2.7% to 5.6% (Fig. 2). The correlation coefficients for interobserver agreement were good (CT ECV ICC 0.943 [95% confidence interval (CI): 0.884 to 0.972]; MR ECV ICC 0.976 [95% CI: 0.951 to 0.989], respectively). The mean pre-T1 value of 16- and 24-week models was significantly higher than that of the pre-modeling (16 weeks vs. pre-modeling, $P < 0.001$; 24 weeks vs. pre-modeling, $P = 0.015$). The pre-T1 value correlates well with CT-derived ECV ($n = 30$; $r = 0.788$; $P < 0.001$) and serum fibrosis index ($n = 30$; $r = 0.783$, 0.811 and 0.805 for HA, LN and PCIII; $P < 0.001$). There was no specific focal LGE in any of the myocardial segments.

Table 1
Summary of demographics.

	Pre-modeling subjects (n = 13)	16-Week models (n = 10)	24-Week models (n = 7)
Demographics			
Weight (kg)	8.4 ± 1.4	7.1 ± 1.2	8.8 ± 0.8
Sex	Female	Female	Female
Heart rate	90.3 ± 15.1	82.3 ± 9.8	83.6 ± 12.5
Hematocrit (%)	48.4 ± 3.4	43.7 ± 3.0*	41.9 ± 6.5#
LV systolic function			
LV ejection fraction (%)	49.9 ± 2.1	44.8 ± 0.8*	41.4 ± 3.0#
End-systolic volume (mL)	12.5 ± 3.9	14.9 ± 0.5	15.8 ± 1.8
End-diastolic volume (mL)	22.9 ± 2.0	27.0 ± 1.0*	27.2 ± 1.9#
Stroke volume (ml)	11.4 ± 1.1	12.1 ± 0.6	11.3 ± 0.8
Cardiac output (ml/min)	684.9 ± 67.9	723.0 ± 44.5	758.6 ± 194.0
Serum fibrosis index			
Hyaluronic acid (ng/ml)	199.0 ± 15.5	288.2 ± 15.6*	408.8 ± 29.6#
Laminin (ng/ml)	235.1 ± 14.3	348.7 ± 17.4*	410.4 ± 12.5#
Type-III procollagen (ng/ml)	103.4 ± 7.4	148.7 ± 7.6*	181.2 ± 9.7#

Values are mean ± SD.
* Pre-modeling subjects vs. 16-week models, $P < 0.05$.
\# Pre-modeling subjects vs. 24-week models, $P < 0.05$.

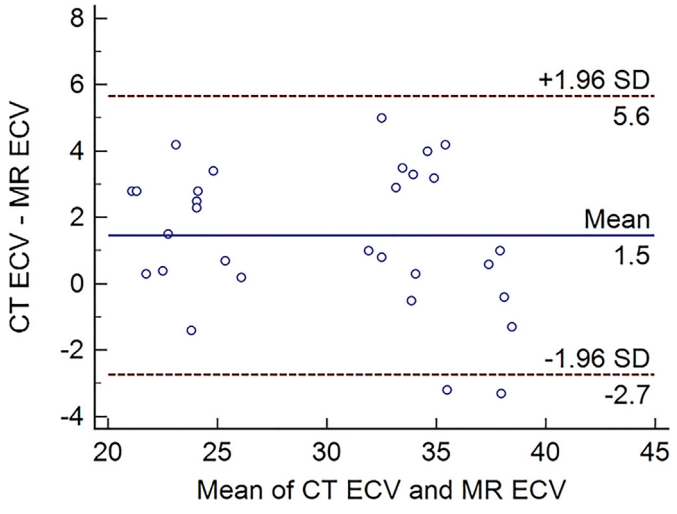

Fig. 2. Bland-Altman Plots for the CT and MR ECV on per beagle analysis. A small bias (1.5%) was noted with 95% limits of agreement from −2.7% to 5.6% between CT and MR ECV.

3.4. Serum fibrosis index

The serum fibrosis index significantly increased with the elongation of modeling time (Table 1). Both CT-derived ECV and MR-derived ECV well correlated with serum fibrosis index (CT ECV vs. HA, LN and PCIII, $r = 0.907$, 0.830 and 0.879, respectively; MR ECV vs. HA, LN and PCIII, $r = 0.852$, 0.753 and 0.824, respectively, all $P < 0.05$). The serum fibrosis index also correlated well with histological CVF values (HA vs. CVF, $r = 0.956$; LN vs. CVF, $r = 0.857$; PCIII vs. CVF, $r = 0.841$, all $P < 0.001$; $n = 13$) (Fig. A.3).

3.5. Histology analysis

Fig. 3 shows the histological results of Masson's trichrome staining in representative beagles from the pre-modeling, 16-week and 24-week modeling groups. CVF increased definitely according to the modeling time (Fig. A.4). Mean CVF values at pre-modeling, 16-week and 24-week groups were 3.6%, 23.1% and 31.9%, respectively. Both the CT-derived ECV and MR-derived ECV correlated well with CVF results ($n = 13$: $r = 0.951$, $P < 0.001$ for CT; $n = 13$: $r = 0.879$, $P < 0.001$ for MR).

3.6. Analysis of other values

The mean pre-T1 value and mean EDV of all post-modeling groups were significantly increased (Tables 1 and A.1). When we used CT-derived ECV, MR-derived ECV, LVEF, serum fibrosis index (HA, LN and PCIII) and EDV for diagnosis of post-modeling groups, the areas under the receiver operating characteristic curve were as follows: 1.000 (95% CI: 1.000 to 1.000) for CT-derived ECV, 1.000 (95% CI: 1.000 to 1.000) for MR-derived ECV, 1.000 (95% CI: 1.000 to 1.000) for LVEF, 1.000 (95% CI: 1.000 to 1.000) for HA, 1.000 (95% CI: 1.000 to 1.000) for LN, 1.000 (95% CI: 1.000 to 1.000) for PCIII, 0.977 (95% CI:0.934 to 1.000) for EDV, respectively. There was no significant difference between these areas under the ROC curve.

4. Discussion

This study investigated 15 beagles including 12 with doxorubicin induced diffuse myocardial fibrosis and 3 pre-modeling histological subjects. ECV fraction was measured with equilibrium contrast-enhanced CT imaging compared to myocardial fibrosis quantified by CMR T1-mapping, serum fibrosis index and histological analysis. Our findings revealed good correlations among CT-derived ECV, MR-derived ECV, serum fibrosis index and histologic CVF, highlighting the reliability of using CCT for quantitative assessment of myocardial tissue changes.

Nowadays, CMR is increasingly used to differentiate the etiology of various cardiomyopathies and ECV derived from CMR has shown promise as a novel biomarker to evaluate diffuse myocardial fibrosis [20]. An increased ECV is most often due to excessive collagen deposition. CMR-derived ECV is less variable and dependent on contrast agent dosing, the delay time after GBCA administration, T1 measurements, and renal clearance [11]. In previous studies, MR-derived ECV measures showed good agreement with histology [18,21–23].

Though MR-derived ECV is a reliable technique for evaluating diffuse myocardial fibrosis, CMR still has some limitations including the associated cost with a CMR examination, the time-consuming acquisition, and certain typical MR-specific contraindications. Considering that iodinated contrast agents for CT are also extracellular interstitial agents, similar to GBCA, CT may provide similar myocardial characterization when substituted for CMR in cases where CMR is either contraindicated or unavailable [24]. CT also offers advantages over MR, including its relative quickness, wider availability and higher spatial resolution [25].

Based on the above theory, a few animal studies have been published. Jablonowski et al. [14] used a myocardial ischemia and reperfusion pig model induced by 16 mm^3 and 32 mm^3 microembolisations. Their findings revealed an excellent correlation between regional ECV using CCT and microscopy ($r^2 = 0.92$). Microscopy measurements also confirmed CCT quantitative measurements and differences in infarct patterns caused by obstruction of major and minor coronary arteries. Hong et al. [15] reported the use of dual-energy CT to characterize myocardial tissue changes in a rabbit model of doxorubicin-induced cardiomyopathy. Their results confirmed that CT-derived ECV and MR-derived ECV values were well correlated ($r = 0.888$; $P < 0.001$). Both techniques also well correlated with histological CVF (CT ECV vs. CVF, $r = 0.925$ and MR ECV vs. CVF, $r = 0.961$, all $P < 0.001$).

These previous animal studies have demonstrated the possibility of quantifying myocardial fibrosis using CCT. However, Jablonowski et al. in their study only focused on myocardial ischemia and infarction models. Hong et al. used dual-energy CT to evaluate doxorubicin-induced DCM and the small heart size and the fast HR or arrhythmia of the rabbits they used in studies may have affected the accuracy of the myocardial tissue assessment. Therefore, aiming to reduce motion artifacts and further verify the reliability of CT ECV, we chose doxorubicin-induced beagles as models of diffuse myocardial fibrosis. The beagle's heart is bigger in size with thicker myocardium compared to the rabbit's heart, and the beagle's HR is slower than that of a rabbit. Different from Hong's study, we used pre-contrast and post-contrast CCT to characterize myocardial tissue. At present, no studies have been published addressing interstitial myocardial fibrosis evaluation with pre-contrast and post-contrast CCT in the setting of drug-induced cardiotoxicity in animals. Furthermore, we analyzed the correlation between CT ECV and serum fibrosis index. Thus, results of this study provide additional value to the existing literature.

Further studies also reported the diagnostic performance of CCT compared to CMR in patients. Nacif et al. [24] studied 24 subjects (11 healthy and 13 with heart failure) to measure ECV using CCT and CMR imaging. They revealed a good correlation in myocardial ECV measurements between CMR and CCT ($r = 0.82$, $P < 0.001$). As expected, ECV was higher in patients with heart failure than in control subjects for both CCT and CMR imaging ($P = 0.03$, respectively). The same group

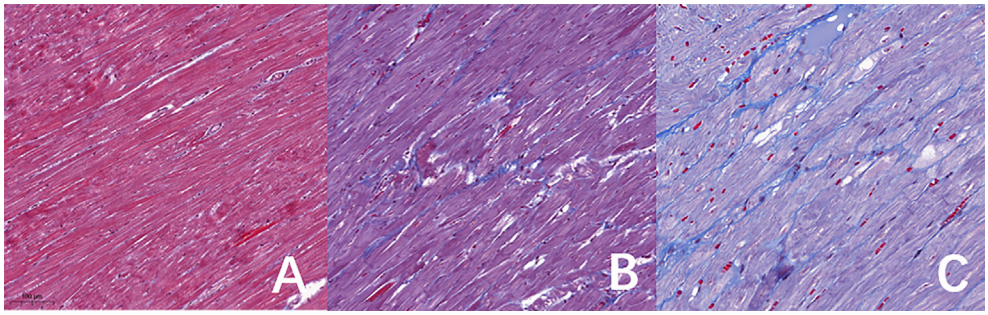

Fig. 3. Representative histological examples. Representative histological examples at pre-modeling (A), 16 (B), and 24 (C) weeks. Masson's trichrome staining (blue = fibrosis, purple = myocardial fibers): With an increasing duration of modeling time, diffuse interstitial fibrosis became increasingly serious and collagen volume fraction values increased (original magnification ×200).

also used a 3-dimensional (3D) approach to derive whole heart ECV. Their findings showed that higher 3D ECV by CCT was associated with reduced systolic circumferential strain, greater EDV and ESV, and lower LVEF ($r = 0.70$, $r = 0.60$, $r = 0.73$ and $r = -0.68$; all $P < 0.001$), suggesting the potential for myocardial tissue characterization using 3D ECV by CCT. In addition, the study of Treibel et al. showed CT derived-ECV was higher in amyloidosis than severe aortic stenosis (AS) (0.54 ± 0.11 vs. 0.28 ± 0.04, $P < 0.001$), and CT derived-ECV results correlated well with CMR derived-ECV ($r^2 = 0.85$ vs. $r^2 = 0.74$) [26]. They also found synthetic CT derived-ECV of these subjects, calculated by synthetic Hct, correlated well with conventional CT derived-ECV ($r^2 = 0.96$; $P < 0.01$), as well as histological CVF ($r^2 = 0.50$, $P < 0.01$). They provided instantaneous quantification of the myocardial extracellular volume without the need for blood sampling, which may contribute to the clinical use of this technique [27]. Based on the results of the Kurita et al., CT derived-ECV showed age-related increase and gender-related difference, enabling CT myocardial fibrosis evaluation in various pathological conditions a part of comprehensive cardiac CT examination [28]. Up to now, few studies have been published addressing interstitial myocardial fibrosis evaluation with CCT in the setting of drug-induced cardiotoxicity, thus further CT studies are needed.

In this study, we find the LVV of the beagles increased and LV systolic function decreased with an increasing duration of modeling time. Similar to other reports, our results revealed an excellent correlation between myocardial ECV by CCT and that by CMR. For both CCT and CMR, ECV was inversely related to LVEF. In addition, we also found a good correlation between CT-derived ECV and serum fibrosis index. The serum fibrosis index also well correlated with CVF. Although the easy lab test can reveal the extent of myocardial fibrosis, the specificity of the serum fibrosis index is poor (other extracardiac sources deserve to be considered) [29]. In contrast, image findings may show earlier findings of fibrosis than the lab test.

Currently, we performed the post-contrast CT acquisitions at 5, 10 and 15 min and post-contrast CMR scans at 15 min to ensure that the contrast agent was evenly distributed in the myocardium. CT-derived ECV values did not significantly change throughout the scanning, which suggests that it may be possible to perform CT-derived ECV in <10 min compared to the 15 min needed to have a reliable ECV estimation with MR exam. Further studies with a larger sample size are needed.

In summary, CT-derived ECV showed high correlations between histological analysis and serum fibrosis index in our study. We demonstrated that CT-derived ECV is a reliable method for detecting diffuse myocardial fibrosis in a doxorubicin-induced beagle model. Equilibrium contrast-enhanced CT seem to be a feasible alternative to CMR for patients with MR contraindications, although radiation exposure risk may limit its clinical application. There are effective radiation dose reduction strategies, such as the use of iterative reconstruction algorithms that are constantly emerging. Our results should be interpreted with caution as this is a preliminary study. Further research on patient's data is necessary to validate these findings.

5. Study limitations

The conventional CT technique used in our study has its inherent limitation with mismatch between pre- and post-contrast scans. For the analyses, ROIs in the myocardial septal and lateral segments were selected based on the post-contrast image, whereas the corresponding areas on the pre-contrast image cannot be fully matched [30]. In order to solve this problem, further studies are required to investigate the ECV at dual-energy CCT. Besides, the small sample size and motion artifacts due to the fast HR may also influence the veracity of results. Although beta-blockers were used, the HR of the beagle is still higher than that of human. Though there are potential advantages of CCT as an imaging technique, such as being faster, less expensive and capable of making myocardial ECV measurements [30], the radiation exposure of CT cannot be ignored.

6. Conclusions

This study demonstrated that equilibrium contrast-enhanced CT-derived ECV is a feasible, noninvasive biomarker for quantitatively measuring diffuse myocardial fibrosis when compared to CMR. Meanwhile, CT-derived ECV showed strong correlations between histological analysis and serum fibrosis index. Thus, CT-derived ECV is expected to be an effective complement to CMR for the assessment of patients with MR contraindications. Larger studies are imperatively needed to verify the reliability of CT-derived ECV. Furthermore, this proof of concepts may be expected to be translated from animal studies to human studies.

Acknowledgment

This study was supported by grants from Natural Science Foundation of China (grants 81641069 and 81271542), and a grant from the Ministry of Science and Technology of the People's Republic of China (2016YFC1300301). We express our sincere appreciation to Kang PuAn Biotechnology Co. Ltd. (Beijing, China) for its collaboration on the histological analysis.

Disclosures of conflicts of interest

Z.Z. disclosed no relevant relationships. L.X. disclosed no relevant relationships. R.W. disclosed no relevant relationships. J.A.D. disclosed no relevant relationships. Z.S. disclosed no relevant relationships. Z.F. disclosed no relevant relationships. U.J.S. is a consultant for and/or receives institutional research support from Astellas, Bayer, GE, and Siemens. A.V.S. receives institutional research support from Siemens.

Appendix A. Supplementary data

Supplementary data to this article can be found online at https://doi.org/10.1016/j.ijcard.2019.01.021.

References

[1] A.S. Flett, M.P. Hayward, M.T. Ashworth, et al., Equilibrium contrast cardiovascular magnetic resonance for the measurement of diffuse myocardial fibrosis: preliminary validation in humans, Circulation 122 (2) (2010) 138–144.
[2] L. Elbl, H. Hrstkova, V. Chaloupka, The late consequences of anthracycline treatment on left ventricular function after treatment for childhood cancer, Eur. J. Pediatr. 162 (10) (2003) 690–696.
[3] H. Arheden, M. Saeed, C.B. Higgins, et al., Measurement of the distribution volume of gadopentetate dimeglumine at echo-planar MR imaging to quantify myocardial infarction: comparison with 99mTc-DTPA autoradiography in rats, Radiology 211 (3) (1999) 698–708.
[4] Daniel R. Messroghli, James C. Moon, Vanessa M. Ferreira, et al., Clinical recommendations for cardiovascular magnetic resonance mapping of T1, T2, T2* and extracellular volume: a consensus statement by the Society for Cardiovascular Magnetic Resonance (SCMR) endorsed by the European Association for Cardiovascular Imaging (EACVI), J. Cardiovasc. Magn. Reson. 19 (1) (2017) 75.
[5] E.B. Schelbert, S.M. Testa, C.G. Meier, et al., Myocardial extravascular extracellular volume fraction measurement by gadolinium cardiovascular magnetic resonance in humans: slow infusion versus bolus, J. Cardiovasc. Magn. Reson. 13 (1) (2011) 16.
[6] D. Radenkovic, S. Weingärtner, L. Ricketts, J.C. Moon, G. Captur, T1 mapping in cardiac MRI, Heart Fail. Rev. 22 (4) (2017) 1–16.
[7] D.R. Messroghli, K. Walters, S. Plein, et al., Myocardial T1 mapping: application to patients with acute and chronic myocardial infarction, Magn. Reson. Med. 58 (1) (2007) 34–40.
[8] P. Sparrow, D.R. Messroghli, S. Reid, J.P. Ridgway, G. Bainbridge, M.U. Sivananthan, Myocardial T1 mapping for detection of left ventricular myocardial fibrosis in chronic aortic regurgitation: pilot study, Am. J. Roentgenol. 187 (6) (2006) 630–635.
[9] A.S. Flett, D.M. Sado, G. Quarta, et al., Diffuse myocardial fibrosis in severe aortic stenosis: an equilibrium contrast cardiovascular magnetic resonance study, Eur. Heart J. Cardiovasc. Imaging 13 (10) (2012) 819–826.
[10] S.M. Banypersad, D.M. Sado, A.S. Flett, et al., Quantification of myocardial extracellular volume fraction in systemic AL amyloidosis an equilibrium contrast cardiovascular magnetic resonance study, Circ. Cardiovasc. Imaging 6 (1) (2013) 34–39.

[11] P. Haaf, P. Garg, D.R. Messroghli, D.A. Broadbent, J.P. Greenwood, S. Plein, Cardiac T1 Mapping and Extracellular Volume (ECV) in clinical practice: a comprehensive review, J. Cardiovasc. Magn. Reson. 18 (1) (2017) 89.
[12] H.J. Lee, D.J. Im, J.C. Youn, et al., Myocardial extracellular volume fraction with dual-energy equilibrium contrast-enhanced cardiac CT in nonischemic cardiomyopathy: a prospective comparison with cardiac MR imaging, Radiology 280 (1) (2016) 49–57.
[13] B.L. Gerber, B. Belge, G.J. Legros, et al., Characterization of acute and chronic myocardial infarcts by multidetector computed tomography: comparison with contrast-enhanced magnetic resonance, Circulation 113 (2006) 823–833.
[14] R. Jablonowski, M.W. Wilson, L. Do, S.W. Hetts, M. Saeed, Multidetector CT measurement of myocardial extracellular volume in acute patchy and contiguous infarction: validation with microscopic measurement, Radiology 274 (2) (2015) 370–378.
[15] Y.J. Hong, T.K. Kim, D. Hong, et al., Myocardial characterization using dual-energy CT in doxorubicin-induced DCM comparison with CMR T1-mapping and histology in a rabbit model, JACC Cardiovasc. Imaging 9 (7) (2016) 836–845.
[16] D.M. Angélica, S.A. Evangelista, F.M.C.T. Dal, C.A. Antonio, Study of the central and peripheral hematologic profile in normal dogs treated with doxorubicin, Braz. J. Morphol. Sci. 14 (2) (1997) 235–241.
[17] S.S. Halliburton, S. Abbara, M.Y. Chen, et al., SCCT guidelines on radiation dose and dose-optimization strategies in cardiovascular CT, J. Cardiovasc. Comput. Tomogr. 5 (4) (2011) 198–224.
[18] M. Zeng, N. Zhang, Y. He, et al., Histological validation of cardiac magnetic resonance T1 mapping for detecting diffuse myocardial fibrosis in diabetic rabbits, J. Magn. Reson. Imaging 44 (5) (2016) 1179–1185.
[19] N.A. Obuchowski, Nonparametric analysis of clustered ROC curve data, Biometrics 53 (2) (1997) 567–578.
[20] J.C. Moon, D.R. Messroghli, P. Kellman, et al., Myocardial T1 mapping and extracellular volume quantification: a Society for Cardiovascular Magnetic Resonance (SCMR) and CMR Working Group of the European Society of Cardiology consensus statement, J. Cardiovasc. Magn. Reson. 15 (1) (2013) 92.
[21] T.G. Neilan, O.R. Coelhofilho, R.V. Shah, et al., Myocardial extracellular volume fraction from T1 measurements in healthy volunteers and mice: relationship to aging and cardiac dimensions, JACC Cardiovasc. Imaging 6 (6) (2013) 672–683.
[22] C.D. de Ravenstein, C. Bouzin, S. Lazam, et al., Histological validation of measurement of diffuse interstitial myocardial fibrosis by myocardial extravascular volume fraction from Modified Look-Locker imaging (MOLLI) T1 mapping at 3 T, J. Cardiovasc. Magn. Reson. 17 (1) (2015) 48.
[23] O.R. Coelho-Filho, R.V. Shah, T.G. Neilan, et al., Cardiac magnetic resonance assessment of interstitial myocardial fibrosis and cardiomyocyte hypertrophy in hypertensive mice treated with spironolactone, J. Am. Heart. Assoc. 3 (3) (2014) e000790.
[24] M.S. Nacif, N. Kawel, J.J. Lee, et al., Interstitial myocardial fibrosis assessed as extracellular volume fraction with low-radiation-dose cardiac CT, Radiology 264 (3) (2012) 876–883.
[25] S. Bandula, S.K. White, A.S. Flett, et al., Measurement of myocardial extracellular volume fraction by using equilibrium contrast-enhanced CT: validation against histologic findings, Radiology 269 (2) (2013) 395–402.
[26] T.A. Treibel, S. Bandula, Marianna Fontana, et al., Extracellular volume quantification by dynamic equilibrium cardiac computed tomography in cardiac amyloidosis, J. Cardiovasc. Comput. Tomogr. 9 (6) (2015) 585–592.
[27] T.A. Treibel, M. Fontana, J.A. Steeden, et al., Automatic quantification of the myocardial extracellular volume by cardiac computed tomography: synthetic ECV by CCT, J. Cardiovasc. Comput. Tomogr. 11 (3) (2017) 221–226.
[28] Y. Kurita, K. Kitagawa, Y. Kurobe, et al., Estimation of myocardial extracellular volume fraction with cardiac CT in subjects without clinical coronary artery disease: a feasibility study, J. Cardiovasc. Comput. Tomogr. 10 (3) (2016) 237–241.
[29] J. Díez, C. Laviades, I. Monreal, et al., Toward the biochemical assessment of myocardial fibrosis in hypertensive patients, Am. J. Cardiol. 76 (13) (1995) 14D–17D.
[30] M.S. Nacif, Y. Liu, J. Yao, et al., 3D left ventricular extracellular volume fraction by low radiation dose cardiac CT: assessment of interstitial myocardial fibrosis, J. Cardiovasc. Comput. Tomogr. 7 (1) (2013) 51–57.